Computing and Informatics, Vol. 28, 2009, 299–318

DUAL-TREE COMPLEX WAVELET TRANSFORM BASED LOCAL BINARY PATTERN WEIGHTED HISTOGRAM METHOD FOR PALMPRINT RECOGNITION

Yanxia Wang

College of Mathematics,Physics and Information Engineering
Zhejiang Normal University
No. 688, Yingbin Road, Jinhua
321004, Zhejiang Province, China
e-mail: `wangyx@zjnu.edu.cn`

Qiuqi Ruan

Institute of Information Science
Beijing Jiaotong University
No. 3 Shang Yuan Cun, Xi Zhi Men
100044, Being, China
e-mail: `qqruan@center.njtu.edu.cn`

Manuscript received 21 June 2007; revised 9 January 2008
Communicated by Steve J. Maybank

Abstract. In the paper, we improve the Local Binary Pattern Histogram (LBPH) approach and combine it with Dual-Tree Complex Wavelet Transform (DT-CWT) to propose a Dual-Tree Complex Wavelet Transform based Local Binary Pattern Weighted Histogram (DT-CWT based LBPWH) method for palmprint representation and recognition. The approximate shift invariant property of the DT-CWT and its good directional selectively in 2D make it a very appealing choice for palmprint representation. LBPH is a powerful texture description method, which considers both shape and texture information to represent an image. To enhance the representation capability of LBPH, a weight set is computed and assigned to the finial feature histogram. Here we needn't construct a palmprint model by a train sample set, which is not like some methods based on subspace discriminant analysis or statistical learning. In the approach, a palmprint image is first decomposed into multiple subbands by using DT-CWT. After that, each subband in complex wavelet domain is divided into non-overlapping sub-regions. Then LBPHs are extracted from each sub-region in each subband, and lastly, all of LBPHs are weighted and concatenated into a single feature histogram to effectively represent the palmprint image. A Chi square distance is used to measure the similarity of different feature histograms and the finial recognition is performed by the nearest neighborhood classifier. A group of optimal parameters is chosen by 20 verification tests on our palmprint database. In addition, the recognition results on our palmprint database and the database from the Hong Kong Polytechnic University show the proposed method outperforms other methods.

Keywords: Biometrics, palmprint recognition, dual-tree complex wavelet transform, local binary pattern, histogram, feature extraction

Mathematics Subject Classification 2000: 68T10 (Pattern identification)

1 INTRODUCTION

With the increasing demand for information security and social security, biometric recognition which uses physiological characteristics of a person to recognize the identity of a person has taken on more importance. Palmprint recognition, as a relatively new branch of biometric recognition, uses the features of palmprints to identify a person, that is, principal lines, wrinkles, ridges, minutiae points, singular points and texture etc. The principal lines and wrinkles in a palmprint convey a large amount of information that can uniquely identify a person and they can be obtained from a low resolution image. Moreover, the features of a palmprint vary very little over time and they are difficult or impossible to be fabricated. Thus, palmprint recognition has received significant attention from research fields and security applications [1, 2, 3, 4].

Comparing with other biometric recognition technologies, limited work has been reported on palmprint recognition, despite the importance of palmprint features. In recent times, some representation approaches have been proposed in the previous work. These methods can be mainly classified into three types: the methods of using structure feature, texture feature and algebraic feature, respectively.

The first type includes the recognition approaches of using point feature and line feature. For instance, Duta [5] defined some points in the principal lines and extracted these points to realize palmprint recognition. Zhang and Shu [6] proposed direction projection algorithm to extract datum features and used improved template algorithm to extract line features. Both invariant datum features and line features were used to identify an individual. X.Q. Wu [7] devised a set of directional line detectors to extract the principal lines and then classified the palmprint by the number of these principal lines and the intersections of these principal lines. These methods demand high quality palmprint images and good feature extraction and matching algorithms.

The second type uses linear discrimination analysis to extract algebraic features of palmprints, such as Eigenpalms [8], Fisherpalms [9], ICA [10]. They all inherently suffer from a generalizability problem: a training procedure is unavoidable. For example, for linear discrimination analysis approaches, in order to seek for the directions which are advantageous for discrimination to represent the final classification, each palmprint image is considered as a point in a high-dimensional image space to construct a training set to compute the discriminant subspace and extract algebraic features of palmprints. However, the discriminant subspace is greatly dependent on the training set. Once the training set is subject to change, the whole training procedure will be repeated. Because of the population explosion and mass migration movements, the generalizablity problem will give rise to a huge bottleneck for most real-work palmprint recognition applications.

The last one includes the methods of using Global Texture Energy(GTE) [11], Fourier transform [12], fuzzy directional element energy feature [13], Gabor filter [14] and wavelet transform [15] etc. Though these methods can easily extract texture features of palmprints, they are not strong enough. In recent years, some statistical learning methods are used to enhance the representation capability of texture descriptors. For example, X. J. Wang [16] proposed a palmprint identification approach using boosting local binary pattern histograms to extract and represent the local features of palmprints. In the method, AdaBoosting algorithm was used to select sub-windows with more discriminative information for classification. G. Y. Chen [17] investigated the application of the dual-tree complex wavelet and support vector machines (SVM) for palmprint classification. By using statistical learning algorithm, texture features based palmprint classification methods are more effective, but they are not entirely independent on the training set.

In order to resolve these problems, we improve the Local Binary Pattern Histogram (LBPH) approach and combine it with Dual-Tree Complex Wavelet Transform (DT-CWT) to propose a dual-tree complex wavelet transform based Local Binary Pattern Weighted Histogram (DT-CWT based LBPWH) method for palmprint recognition. In the method, a palmprint image is transformed into complex wavelet domain by a DT-CWT and a number of decomposition levels of the palmprint image are obtained. In each decomposition level, there are six subbands in different orientations. To obtain more useful texture information from these subbands, each of them is divided into multiple non-overlapping sub-regions and sub-histograms are extracted from each labelled sub-region by a LBP operator independently. Finally, these sub-histograms are weighted and concatenated into a single feature histogram to represent the palmprint image. For classification, histogram intersection method is used to measure the similarity of feature histograms of different palmprint images. Therefore, a training procedure is unnecessary to construct palmprint model in the proposed method, that is, the method is entirely independent on the training set. 20 verification tests on our palmprint database are used to choose a group of optimal parameters for the proposed method. In addition, the recognition results on our palmprint database and the database from the Hong Kong Polytechnic University show the proposed method outperforms other methods.

The rest of the paper is organized as follows: A brief description of dual-tree complex wavelet transform is given in Section 2. Section 3 describes local binary pattern method and the dual-tree complex wavelet transform based local binary pattern weighted histogram method in detail. Section 4 reports the experimental results and analysis. Finally, the conclusion is given in Section 5.

2 DUAL-TREE COMPLEX WAVELET TRANSFORM

Wavelet techniques are successfully applied to various problems in image processing and pattern recognition. However, a major problem of the common decimated Discrete Wavelet Transform (DWT) is its lack of shift invariance. This means that on shifts of the input signal, the wavelet coefficients vary substantially. However, the property of shift invariance is very important in invariant pattern recognition. Because complex wavelet transform does not suffer from the problem, it can be a simple solution to the shortcoming of DWT. However, traditional formulations of complex wavelets are seldom used because they generally suffer from either lack of speed or poor inversion properties [18]. Fortunately, Kingsbury [19, 20] developed DT-CWT to solve these two fundamental problems while retaining the properties of nearly shift invariance and directionally selectivity in two and higher dimensions that complex wavelets provide. Dual-tree complex wavelet transform attains these properties by replacing the tree structure of the conventional wavelet transform with a dual tree. He proposed a simple delay of one sample between level 1 filters in each tree, and then the use of linear-phase filters with alternate odd-length and even-length; but he pointed out that there are some problems with the odd/even filter approach. Thus, he proposed a new Q-shift dual-tree [21]; the structure of 1D Q-shift dual-tree is shown in Figure 1.

In the course of implementation of DT-CWT, there are tow sets of filters used, the one set of filters at level 1, and the other set of filters at all higher levels. The filters beyond level 1 have even length but are no longer strictly linear phase and have a group delay of approximately 1/4. The required delay difference of 1/2 sample is achieved by using the time reverse of the tree and filters in tree b. At each scale one tree produces the real part of the complex wavelet coefficients, while the other produces the imaginary parts. Note that dual-tree complex wavelet transform employs two real DWTs in essence, and complex coefficients only appear when the two trees are combined. DT-CWT has the following properties:

1. nearly shift invariance;
2. good selectivity and directionality in 2D (or higher dimension) with Gabor-like filters;
3. perfect reconstruction (PR) using short linear phase filters;

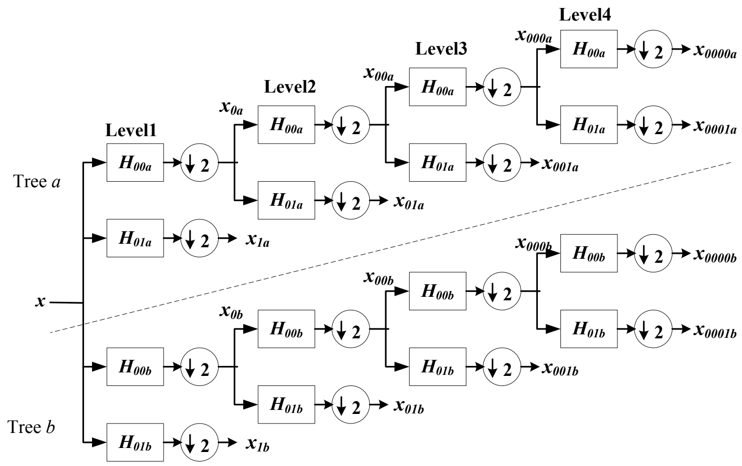

Fig. 1. The 1D Q-shift dual tree structure [21]

4. limited redundancy, independent of the number of scales, for example, a redundancy factor of only 2^m for m-dimensional signals;

5. efficient order-N computation: only 2^m times the simple real DWT for m-dimensional signal.

The multidimensional DT-CWT is non-separable but is based on a computationally efficient, separable filter bank (FB). A 2D dual-tree complex wavelet can be defined as $\psi(x,y) = \psi(x)\psi(y)$ associated with the row-column implementation of the wavelet transform, where $\psi(x)$ and $\psi(y)$ are two complex wavelets, $\psi(x) = \psi_h(x) + j\psi_g(x)$ and $\psi(y) = \psi_h(y) + j\psi_g(y)$, $\psi_h(\bullet)$ and $\psi_g(\bullet)$ are real wavelet transforms of upper FB and lower FB, respectively. Then we obtain the following for the expression [22]:

$$\begin{aligned}\psi(x,y) &= [\psi_h(x) + j\psi_g(x)][\psi_h(y) + j\psi_g(y)] \\ &= \psi_h(x)\psi_h(y) - \psi_g(x)\psi_g(y) + j[\psi_g(x)\psi_h(y) + \psi_h(x)\psi_g(y)].\end{aligned} \tag{1}$$

A 2D DT-CWT is oriented and approximately analytic at the cost of being four-times expansive. It also possesses the full shift-invariant properties of the constituent 1D transforms. The real parts of six oriented complex wavelets of DT-CWT can be defined as follows:

$$\begin{aligned}\varphi_i(x,y) &= \tfrac{1}{\sqrt{2}}(\psi_{1,i}(x,y) - \psi_{2,i}(x,y)) \\ \varphi_{i+3}(x,y) &= \tfrac{1}{\sqrt{2}}(\psi_{1,i}(x,y) - \psi_{2,i}(x,y))\end{aligned} \tag{2}$$

where $i = 1, 2, 3$ and

$$\begin{aligned}
\psi_{1,1}(x,y) &= \phi_h(x)\psi_h(y) \qquad & \psi_{2,1}(x,y) &= \phi_g(x)\psi_g(y) \\
\psi_{1,2}(x,y) &= \psi_h(x)\phi_h(y) \qquad & \psi_{2,2}(x,y) &= \psi_g(x)\phi_g(y) \\
\psi_{1,3}(x,y) &= \psi_h(x)\psi_h(y) \qquad & \psi_{2,3}(x,y) &= \psi_g(x)\psi_g(y).
\end{aligned} \tag{3}$$

The imaginary parts of six oriented complex wavelets of DT-CWT can be defined as follows:

$$\begin{aligned}
\xi_i(x,y) &= \tfrac{1}{\sqrt{2}}(\psi_{3,i}(x,y) - \psi_{4,i}(x,y)) \\
\xi_{i+3}(x,y) &= \tfrac{1}{\sqrt{2}}(\psi_{3,i}(x,y) - \psi_{4,i}(x,y))
\end{aligned} \tag{4}$$

where $i = 1, 2, 3$ and

$$\begin{aligned}
\psi_{3,1}(x,y) &= \phi_g(x)\psi_h(y) \qquad & \psi_{4,1}(x,y) &= \phi_h(x)\psi_g(y) \\
\psi_{3,2}(x,y) &= \psi_g(x)\phi_h(y) \qquad & \psi_{4,2}(x,y) &= \psi_h(x)\phi_g(y) \\
\psi_{3,3}(x,y) &= \psi_g(x)\psi_h(y) \qquad & \psi_{4,3}(x,y) &= \psi_h(x)\psi_g(y).
\end{aligned} \tag{5}$$

In Equations (3) and (4), $\phi_h(\bullet)$ and $\phi_g(\bullet)$ are the low-pass functions of upper FB and lower FB, respectively along the first dimension. $\psi_h(\bullet)$ and $\psi_g(\bullet)$ are the high-pass functions of upper FB and lower FB, respectively along the second dimension. A 2D DT-CWT produces three subbands in each of spectral quadrants 1 and 2, giving six subbands of complex coefficients at each level, which are strongly oriented at angles of $\pm 15^o, \pm 45^o, \pm 75^o$ as shown by their impulse responses in Figure 2 [19].

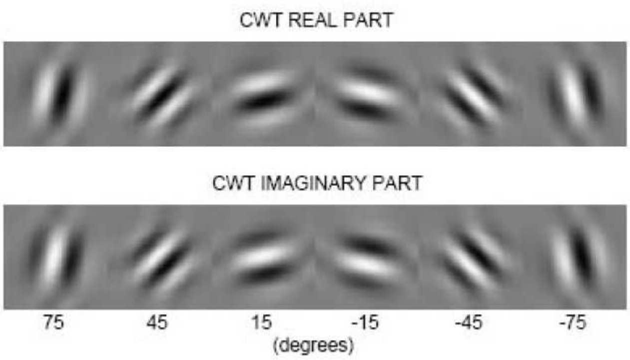

Fig. 2. The 2D impulse responses of the dual-tree complex wavelets at level 4

3 DUAL-TREE COMPLEX TRANSFORM BASED LOCAL BINARY PATTERN WEIGHTED HISTOGRAM METHOD

To further enhance the capability in characterizing different classes of palmprints, each subband of the DT-CWT can be further encoded. Local binary pattern his-

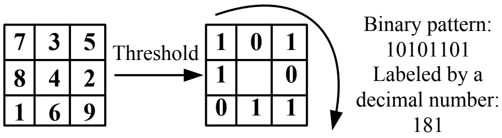

Fig. 3. The basic LBP operator

togram is a nonparametric method in nature and is an effective texture descriptor. It has been applied successfully in texture analysis and recognition [23, 24, 25].

3.1 Local Binary Pattern Histogram

The basic LBP histogram method, introduced by Ojala et al. [26], is defined as a gray-scale invariant texture measure, derived from a general definition of texture in a local neighborhood. Firstly, the LBP operator labels the pixels of an image by thresholding the 3×3-neighborhood of each pixel with the center value and the result as a binary number. Then a decimal number of the binary number is used to label the center pixel. At last, the histogram of the labels can be used as a texture descriptor. Figure 3 shows the illustration of the basic LBP operator.

Later the operator was extended in two aspects [27]. The extended LBP operator uses neighborhoods of different sizes and shapes to label each pixel by bilinear interpolation. Because of using circular neighborhood and bilinear interpolation, any radius and number of pixels are chosen in the neighborhood. For neighborhoods we will use the notation (N, ρ) which means N sampling points on a circle of radius of ρ. Figure 4 shows some examples of the circularly symmetric neighborhoods. Another extension to the original operator uses the certain local binary pattern termed "uniform patterns". A LBP is called uniform if it contains at most tow bitwise transitions or discontinuities from 0 to 1 or vice versa in the circular presentation of the pattern. The improved operator not only possesses a property of gray-scale and rotation invariant operator, but also allows for detecting "uniform pattern" at circular neighborhoods of any quantization of the angular space and at any spatial resolution. Both the two properties are important for palmprint recognition.

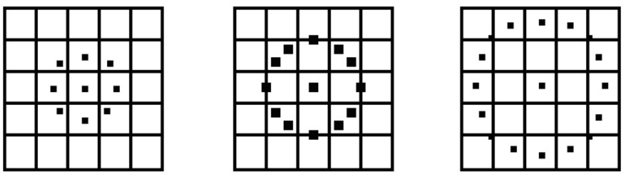

Fig. 4. Circularly symmetric neighbor sets of different (N, ρ)

The "uniform pattern" can be denoted as $LBP^{riu2}_{N,\rho}$:

$$LBP^{riu2}_{N,\rho} = \begin{cases} \sum\limits_{p=0}^{N-1} s(g_p - g_c), & if \quad U(LBP_{N,\rho}) \leq 2 \\ N+1 & otherwise \end{cases} \tag{6}$$
$$U(LBP_{N,\rho}) = |s(g_{N-1} - g_c) - s(g_0 - g_c)| + \sum_{p=0}^{N-1} |s(g_p - g_c) - s(g_{p-1} - g_c)|$$

where superscript ^{riu2} reflects the use of rotation invariant "uniform" patterns, $s(\bullet)$ is a sign function, g_c is the gray value of the center pixel of the local neighborhood and $g_p(p = 0, \cdots, N-1)$ is the gray value of equally spaced pixels on the circle. By Equation (6), the value of U(LBP$_{N,\rho}$) of every pixel in an image is computed to label the image.

After labeling all of the pixels of the image, a histogram of the labeled image can be defined as

$$H_i = \sum_{x,y} I\{f_l(x,y) = i\} \qquad i = 0, \cdots, n-1 \tag{7}$$

where n is the number of different labels produced by the $LBP^{riu2}_{N,\rho}$ operator and $IA = 1$ if A is true, 0 otherwise. This histogram contains information about the distribution of the local micropatterns, such as edges, spots and flat areas, over the whole image.

3.2 Dual-Tree Complex Wavelet Transform Based Local Binary Pattern Weighted Histogram Method

3.2.1 Basic Idea

Because a palmprint image is a low resolution image, instead of directly using the intensity to compute the spatial histogram, a multi-level and multi-direction DT-CWT is used for the decomposition of a palmprint image. Several decomposition levels of the palmprint image are obtained, and there are six subbands in each decomposition level. The value of U(LBP$_{N,\rho}$) of every magnitude of complex coefficients in these subbands is computed by a LBP operator to label the subbands. After labeling all of the magnitudes of complex coefficients in a subband, the subband becomes a labeled subband. By combining DT-CWT and LBPH methods, the representation power of the spatial histogram is enhanced greatly.

Moreover, though LBPH method is an effective method for texture representation, because palm lines in the image are lines with irregular directions and various depth, it may cause the loss of spatial information to use the feature histogram extracted from the whole labeled subbands to describe a palmprint. Thus each labeled subband is divided into multiple non-lapping sub-regions and the corresponding histograms extracted from these sub-regions are called "sub-histograms".

In addition, when a subband has been divided into multiple sub-regions, it can be expected that some of the sub-regions contain more information than others in terms of distinguish between people. For example, principal lines seem to be an important cue in palmprint recognition [30]. The sub-regions concluding a part of principal lines contain more information than the sub-regions without palm lines. Thus, a weight can be set for each sub-region based on the importance of the information it contains.

Considering the above factors, an effective palmprint representation and recognition method, DT-CWT based LBPWH, is developed by improving the local binary pattern method and combining it with the dual-tree complex wavelets transform. Figure 5 shows the block of proposed method.

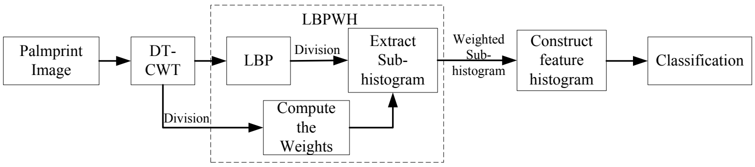

Fig. 5. The block of DT-CWT based LBPWH method

3.2.2 Local Binary Pattern Weighted Histogram Method

A labeled subband of DT-CWT of a palmprint image in l^{th} level and d^{th} direction can be denoted as $M_{l,d}^{lab}(x,y)$, a histogram of $M_{l,d}^{lab}(x,y)$ can be defined as

$$H_{l,d,i} = \sum_{x,y} I\{M_{l,d}^{lab}(x,y) = i\}, \quad l = 1, \cdots, L, \;\; d = 1, \cdots, 6, \;\; i = 0, \cdots, n-1. \tag{8}$$

Here L is the total number of the levels of DT-CWT, definitions of n and i are the same as the definition in Equation (7). In the pursuit of more efficient representation, each $M_{l,d}^{lab}(x,y)$ in the l^{th} level is divided into m_l sub-regions $R_1, R_2, \ldots, R_{m_l}$, where $m_l = \frac{S_I}{(2^{2l}S_R)}$, S_I is the size of the original palmprint image, S_R is the size of these sub-regions. Then the sub-histogram of the ${r_{l,d}}^{\text{th}}$ region of $M_{l,d}^{lab}(x,y)$ is defined as

$$\begin{aligned} H_{l,d,r_{l,d}} &= (h_{l,d,r_{l,d},0}, h_{l,d,r_{l,d},1}, \cdots, h_{l,d,r_{l,d},n-1}) \\ h_{l,d,r_{l,d},i} &= \sum_{x,y \in R_{r_{l,d}}} I\{M_{l,d}^{lab}(x,y) = i\}, \quad r_{l,d} = 1, 2, 3, \cdots, m_l. \end{aligned} \tag{9}$$

Different sub-regions in a same subband or different subbands are of different importance for palmprint representation and recognition. Consequently the sub-histograms extracted from different sub-regions of $M_{l,d}^{lab}(x,y)$ have different discriminative ability. Therefore, in the method, a weight set can be computed by the magnitudes of DT-CWT and the weights in the set are distributed to different sub-histograms. A weight of the sub-histogram of the $r_{l,d}^{\text{th}}$ sub-region in the l^{th} level and d^{th} direction, $W_{l,d,r_{l,d}}$, can be defined as:

$$W_{l,d,r_{l,d}} = C_l q(d, r_{l,d}|l) b(r_{l,d}|l, d) \tag{10}$$

$$C_l = \begin{cases} \frac{1}{2^l}, & l \le L-1 \\ 1 - \sum\limits_{k=1}^{L-1} \frac{1}{2^k}, & l = L \end{cases} \tag{11}$$

$$b(r_{l,d}|l,d) = \frac{V(l,d,r_{l,d})}{\sum\limits_{r_{l,d}\in(l,d)} V(l,d,r_{l,d})} \tag{12}$$

$$q(d,r_{l,d}|l) = \frac{V(l,d,r_{l,d})}{\sum\limits_{d=1}^{6} V(l,d,r_{l,d})} \tag{13}$$

$$V(l,d,r_{l,d}) = Radon(r_{l,d},\alpha), \alpha = -75^o + 30^o \times (d-1) \tag{14}$$

where C_l is the whole l^{th} level weight, d is the number of the directions of DT-CWT, α is the corresponding direction angle of d, $V(l,d,r_{l,d})$ is the value of Radon transform of sub-region $r_{l,d}$ in the subband (l,d) for the angle α. $b(r_{l,d}|l,d)$ is the weight of sub-region $r_{l,d}$ in a same subband (l,d). $q(d,r_{l,d}|l)$ is the weight of sub-region $r_{l,d}$ in a same level and different subbands. The sketch map of computing $b(r_{l,d}|l,d)$ and $q(d,r_{l,d}|l)$ is shown in Figure 6.

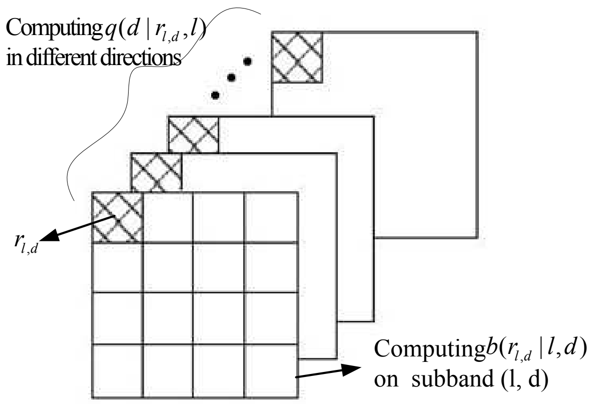

Fig. 6. The sketch map of computing $b(r_{l,d}|l,d)$ and $q(d,r_{l,d}|l)$

$W_{l,d,r_{l,d}}$ is defined as the product of C_l, $b(r_{l,d}|l,d)$ and $q(d,r_{l,d}|l)$. If the value of $b(r_{l,d}|l,d)q(d,r_{l,d}|l)$ of some sub-regions is larger than that of other sub-regions, we can conclude that these sub-regions are more important for recognition, that is, the sub-histograms extracted from these sub-regions have better discriminative ability.

Then the weighted sub-histogram can be defined as

$$wH_{l,d,r_{l,d}} = W_{l,d,r_{l,d}} H_{l,d,r_{l,d}}. \tag{15}$$

Finally, all of the weighted sub-histograms are concatenated to a feature histogram vector, K, to represent a palmprint image

$$K = (wH_{1,1,1}, \cdots, wH_{1,1,m_1}, wH_{1,2,1}, \cdots, wH_{1,2,m_1}, \cdots, \\ wH_{1,6,m_1}, \cdots, wH_{2,1,1}, \cdots, wH_{2,6,m_2}, \cdots, wH_{L,6,m_L}). \tag{16}$$

3.2.3 Implementation of Proposed Method

In our proposed method, a palmprint image is modeled as a feature histogram vector by the following steps:

1. A palmprint image is transformed into complex wavelet domain by an N-level dual-tree complex transform. The palmprint image is decomposed into N levels and $6N$ subbands are obtained.
2. Every magnitude of the complex coefficient in each subband is labeled by the value of $\mathrm{U}(\mathrm{LBP}_{N,\rho})$ computed by Equation (6).
3. Each labeled subband is divided into multiple non-overlapping rectangle sub-regions, and a sub-histogram is extracted from each sub-region.
4. Each subband is also divided into multiple non-overlapping sub-regions as the same as the corresponding labeled subband, and the weights of different sub-regions are computed by Equation (10).
5. The weighted sub-histogram of each sub-region is obtained by Equation (15).
6. All of the weighted sub-histograms are connected to form the final feature histogram to represent the palmprint image.
7. Chi square statistic $\chi^2(K^1K^2)$ is used to measure the similarity of two feature histograms.
8. Finally, a nearest neighbor classifier is used for palmprint classification.

3.2.4 Comparison of Gabor Wavelet Transform and Dual-Tree Complex Wavelet Transform

The properties of DT-CWT, especially nearly shift-invariant and directional selectivity, make it become a very attractive choice for palmprint representation and recognition. Gabor wavelet transform is an effective method for feature extraction of palmprint, and it is frequently applied in palmprint identification [1, 14, 28]. But, the 2D DT-CWT has one advantage over Gabor wavelet transform: the DT-CWT has a smaller redundancy for an image and needs less storage space.

For example, we can compare Gabor wavelet transform with DT-CWT for a palmprint image with the size of 128×128. Figure 7 shows the subbands of Gabor wavelet transform and DT-CWT for the palmprint image. Form Figure 7, we can find that the magnitudes of DT-CWT in the subbands are similar with that of Gabor transform. However, the redundancy of 2D DT-CWT is 4 (2^2, $m = 2$), while Gabor transform with four levels and six directions produces twenty-four subbands with the size 128×128, that is, the redundancy of Gabor wavelet transform

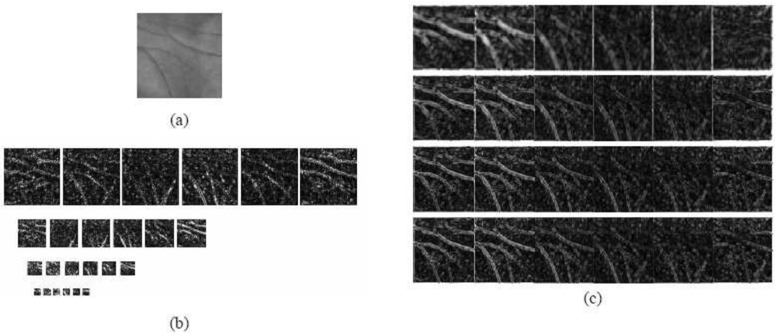

Fig. 7. Comparison of the magnitudes of Gabor wavelet transform and DT-CWT. a) is a palmprint image from our database. b) is the subbands of DT-CWT from level 1 to level 4 in the same six directions. c) is the subbands of Gabor wavelet transform in 4 frequency scales and 6 equal directions.

is 24. In addition, a 2D DT-CWT with the same number of levels and directions also produces 24 subbands, but their sizes are 64×64, 32×32, 16×16 and 8×8 in the different levels from 1 to 4, respectively, which are much smaller than that of Gabor wavelet transform. Thus, less storage spaces are needed and higher execution speed of the application system is obtained. Thus, CT-DWT is a good candidate to replace Gabor transform in palmprint representation and recognition.

4 EXPERIMENTAL RESULTS

4.1 Experimental Data

In this paper, we develop a scanner-based device to capture palm images. The scanner is a Fujitsu fi-60F high speed flatbed scanner, and it is enclosed in an organic glass box. The device is used to capture images of both hands from 150 individuals. The device has not fixed pegs to restrict the palm movement, rotation and stretch. It only uses two bars in each side of the box to avoid the hand removing the scanning area. Ten images are captured from each hand of a person. The palm images are 292×413 pixels with the resolution of 72 dpi in 8-bit gray levels. The center part of each palm is extracted and stored as palmprint images of size 128×128. The total of 3 000 palmprint images ($150 \times 2 \times 10$) form our palmprint database. Figure 8 shows the palmprint capture device, one palm image captured by the device and a palmprint image extracted from the palm image in our database.

4.2 Parameter Selection and Performance Test

In the proposed method, there are some parameters that need to be chosen to optimize the performance of the algorithm. They are the size of the sub-regionS_R,

(a) (b) (c)

Fig. 8. Palmprint capture device, a palm image and its palmprint image in our database

the number of sampling points N and the circle of radius ρ of the $\mathrm{LBP}_{N,\rho}$ operator, and the number of levels of DT-CWT n. Here, n decides the number of subbands, that is to say, a palmprint image is decomposed into $6n$ subbands by using n-level DT-CWT. To obtain best parameters for the proposed method, five different sets of parameters listed in Table 1 are used to test the performance of the proposed method. Four groups of parameters are included in each set of parameters. For example, for $n = 4$, the palmprint image is first decomposed by using 4-level DT-CWT, and 24 subbands are obtained. After that, LBP operator with parameter of (N, ρ) is applied to label these 24 subbands. All subband images are then partitioned into several non-overlapping sub-regions of size S_R, and the weighted histograms of these sub-regions are obtained and connected to form the global feature of the palmprint.

In total, 20 verification tests are carried out for testing these parameters in our palmprint database. For every verification test, the total number of matchings is 8 997 000. 27 000 of them are correct matchings and the rest of them are incorrect matchings. The performance of different groups of parameters is presented by ROC curves. Figures 9 a)–e) show the ROC curves generated by our method with different parameters, and Table 2 summarizes the equal error rate (EER) of the corresponding 20 different parameters groups.

From Table 2 we can find that the mean value of the EERs in the first parameters set (0.4075 %) is smaller than that of other parameters sets (0.7325 %, 1.275 %, 1.0275 %, 1.8925 %). Hence, the proposed method with 4-level DT-CWT is better than the method with 3-level and with 2-level. It is because using 4-level DT-CWT in our method can obtain more subbands and useful information in the palmprint image.

In addition, we can also find that, in the situation of having the same number of levels, the EERs of the proposed method with 8×8 sub-regions are smaller than that of the method with 16×16 sub-regions.

According to Figure 9, it can be found that the ROC curves of (16, 2) in Figure 9 a), b), d) and e) are below that of (8, 1), (8, 2) and (16, 3). Thus, the circular neighborhood (16, 2) has an appropriate radius and the number of sampling points to represent the local information. Because the EER of the proposed method with 4 levels, the 8×8 sub-regions and (16, 2) circular neighborhood is 0.06 %, which is smaller than that of other 19 groups of parameters, the group of parameters is chosen to be used in the proposed method.

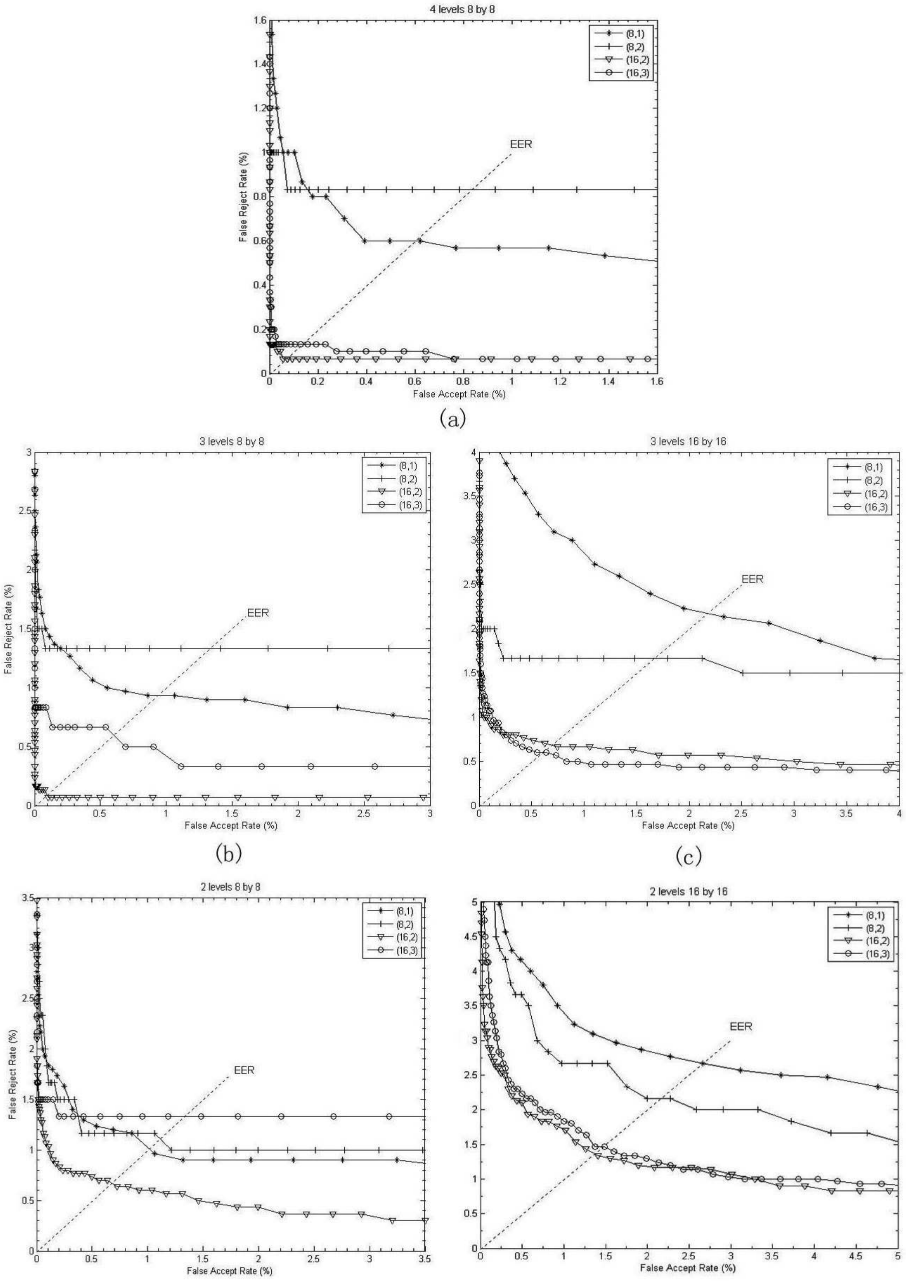

Fig. 9. Verification test results. a)–e) are the ROC curves of the proposed method with parameters sets 1, 2, 3, 4 and 5, respectively.

Set	Group	n	(N, ρ)	S_R	Set	Group	n	(N, ρ)	S_R
1	1	4	(8, 1)	8×8	4	13	2	(8, 1)	8×8
	2	4	(8, 2)	8×8		14	2	(8, 2)	8×8
	3	4	(16, 2)	8×8		15	2	(16, 2)	8×8
	4	4	(16, 3)	8×8		16	2	(16, 3)	8×8
2	5	3	(8, 1)	8×8	5	17	2	(8, 1)	16×16
	6	3	(8, 2)	8×8		18	2	(8, 2)	16×16
	7	3	(16, 2)	8×8		19	2	(16, 2)	16×16
	8	3	(16, 3)	8×8		20	2	(16, 3)	16×16
3	9	3	(8, 1)	16×16					
	10	3	(8, 2)	16×16					
	11	3	(16, 2)	16×16					
	12	3	(16, 3)	16×16					

Table 1. The sets of parameters used to verification test

Set	Group	EER	Mean EER	Set	Group	EER	Mean EER
1	1	0.6 %	0.4075 %	4	13	1.02 %	1.0275 %
	2	0.83 %			14	1.1 %	
	3	0.06 %			15	0.64 %	
	4	0.14 %			16	1.35 %	
2	5	0.92 %	0.7325 %	5	17	2.62 %	1.8925 %
	6	1.31 %			18	2.16 %	
	7	0.1 %			19	1.36 %	
	8	0.6 %			20	1.43 %	
3	9	2.18 %	1.275 %				
	10	1.62 %					
	11	0.7 %					
	12	0.6 %					

Table 2. The EER of the proposed method based on different parameters

4.3 Comparisons with Other Methods

4.3.1 Accuracy Test

In the experiment, the proposed method is tested on our palmprint database (DBI) and on the palmprint database from the Hong Kong Polytechnic University (DBII), respectively. DBII contains 100 different palms, and each has six samples collected in two sessions. Figure 10 shows a palm image and a palmprint image extracted form the palm image. The results of the proposed method on both databases are compared with the results of boosting LBP method [16], DT-CWT method [17], Local Gabor Binary Pattern Histogram Sequence (LGBPHS) method [29] and DT-CWT based LBPH (LCBPH) method, and these results are reported in Table 3.

Compared with the results of different methods on DBI and DBII, it can be found that the results of all of methods on DBI are better than the results on

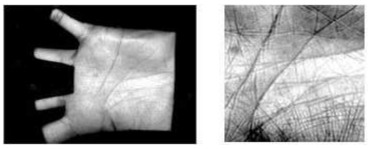

Fig. 10. A palm image and an extracted palmprint image in DBII

Methods	[17]	[16]	[29]	LCBPH	Our method
DBI	98 %	96.5 %	98.67 %	98.5 %	99.67 %
DBII	97 %	97 %	98.25 %	98 %	99.25 %

Table 3. Recognition rates of different methods on DBI and DBII

DBII except the result of the boosting LBP method. It may be because a more symmetrical light is provided by our palmprint capture device and a better quality palmprint image is obtained (Figures 8, 10). But, our capture device has not fixed pegs, and thus the location precision during the extraction of palmprint image and consequently the recognition rate of the boosting LBP method are affected directly. Hence the recognition rate of the method on DBI (96.5 %) is slightly lower than that of the method on DBII (97 %).

In addition, for a same database, we can find that LCBPH method can obtain better recognition rate (98.5 %), which is higher than that of DT-CWT method (98 %) and boosting LBP (96.5 %) on DBI. The same is true on the DBII. Hence, the performance of the combining DT-CWT and LBP operator is better than that of only using one of the tools.

Though DT-CWT is similar to Gabor wavelet transform and can save the storage spaces (see Section 3.2.4), from Table 3 we can find that the LGBPHS method can obtain a better accuracy than the LCBPH method. It is because the redundancy of Gabor wavelet transform is larger than that of DT-CWT, it can get more useful information for identification, which is missing with DT-CWT.

However, a high accuracy of 99.67 % is obtained by the proposed method on DBI. In our method, different weights are computed and assigned to different histograms extracted from different sub-regions to enhance the discriminative ability of the final feature histogram vector. Therefore, our method possesses the advantage of DT-CWT based LBPH method and gets better performance than LGBPHS.

4.3.2 Speed Test

Speed is another factor in determining the efficiency of an algorithm. The proposed approach and other four methods are implemented using Matlab 7.3 on a personal computer with Intel Pentium processor (2.8 GHz). Table 4 lists the average execution time of different methods. In the table, T_1 is the average execution time for training per palmprint image, defined as the ratio of the execution time for training to the number of palmprint images in the train set. T_2 is the average execution time for feature extraction and matchings. T is the total execution time for recognition. D is the times of repetitive training. Because a training procedure is included in the methods proposed by Wang[16] and Chen [17], the average execution time for training per palmprint image T_1 must be worked out as a part of the total execution time of the two methods. It can be found from Table 4 that the total execution time of LCBPH method is less than that of LGBPHS method. It means that the execution speed of DT-CWT is faster than that of Gabor wavelet transform. In our method, time has to be taken to compute the weight for the histograms, so the total execution time of our method is more than that of DT-CWT method. Even so, the total execution time of our method is 0.96 second, which is fast enough for real-time verification.

In addition, DT-CWT method and boosting LBP method spend little time to extract and match features, but, increasing as the times of repetitive training D, the total execution time of the two methods will be further increased. However, for the above two methods, once the train set is changed, the repetitive training procedure is inevitable. When the training procedure is repeated twice, the total execution time of the DT-CWT method is summed to 1.43 second, which is more by 0.47 second than that of our method. Thus, considering the various factors, our method applied in palmprint recognition gives satisfying performance.

Time	[17]	[16]	[29]	LCBPH	Our method
T_1	0.52 s	0.12 s	–	–	–
T_2	0.39 s	0.48 s	1.13 s	0.85 s	0.96 s
T	$(0.39 + 0.52 * D)$ s	$(0.48 + 0.12 * D)$ s	1.13 s	0.85 s	0.96 s

Table 4. Execution time of different methods on DBI

5 CONCLUSIONS

The paper reports a dual-tree wavelet transform based local binary patter weighted histogram method for palmprint recognition. The method combines two effective texture analysis tools to represent and recognze palmprints. Moreover, using the local directional characteristics and significance of different sub-regions of palmprint to compute a weight set to improve the discriminative ability of the final histogram vector. On the basis of the above work, a training procedure is unnecessary to construct palmprint model in our approach, that is, the method is entirely independent on the training set. Verification tests on our palmprint database are used to choose a group of optimal parameters for the proposed method. The proposed method with these appropriate parameters is used to perform accuracy test on our palmprint database and the palmprint database from the Hong Kong Polytechnic University, and the experimental results are compared with those of other methods. In addition, a speed test is designed to discuss the cost of implementation of the proposed method. The experimental results demonstrate that the proposed approach can give a better performance. In summary, the dual-tree wavelet transform based local binary patter weighted histogram method is an effective approach for palmprint recognition.

Acknowledgment

This work is supported partly by the National Grant Fundamental Research 973 Program of China (No. 2004CB318005) and the National Natural Science Foundations of China (No. 60472033 and No. 60672062).

REFERENCES

[1] Zhang, D.—Wai-Kin, K.: Online Palmprint Identification. Pattern Analysis and Machine Intelligence, Vol. 25, 2003, No. 9, pp. 1041–1050.

[2] Wu, X. Q.—Zhang, D.: Palmprint Recognition Using Valley Features. Proceedings of 4th International Conference, ML C '05, Guangzhou, China, Vol. 8, Aug. 2005, pp. 4881–4885.

[3] Kumar, A.—Jain, A. K.: Personal Verification Using Palmprint and Hand Geometry Biometric. Proceedings of the 4th International Conference, AVBPA '03, Guildford, UK, June 2003, pp. 668–675.

[4] Zhang, D.: Palmprint Authentication. Kluwer Academic Publishers, USA, 2004.

[5] Duta, N.—Jain, A. K.: Matching of Palmprints. Pattern Recognition Letters, Vol. 23, 2002, No. 4, pp. 477–485.

[6] Zhang, D.—Shu, W.: Two Novel Characteristics in Palmprint Verification: Datum Point Invariance and Line Feature Matching. Pattern Recognition, Vol. 33, 1999, No. 4, pp. 691–702.

[7] Wu, X. Q.— Zhang, D.: Palmprint Classification Using Principal Lines. Pattern Recognition, Vol. 37, 2004, No. 10, pp. 1987–1998.

[8] Lu, G.—Zhang, D.: Palmprint Recognition Using Eigenpalms Features. Pattern Recognition Letters, Vol. 24, 2003, pp. 1463–1467.

[9] Wu, X.—Zhang, D.: Fisherpalms Based Palmprint Recognition. Pattern Recognition Letters, Vol. 24, 2003, pp. 2829–2838.

[10] Connie, T.: An Automated Palmprint Recognition System. Image and Vision Computing, Vol. 23, 2005, No. 5, pp. 501–515.

[11] Li, W. X.—Zhang, D.: A Texture-based Approach to Palmprint Retrieval for Personal Identification. Proceedings of International Conference, SRMD '2000, San Jose, California, USA, Jan. 2000, pp. 415–424.

[12] Li, W. X.— Zhang, D.: Palmprint Identification by Fourier Transform. International Journal of Pattern Recognition and Artificial Intelligence, Vol. 16, 2002, No. 4, pp. 417–432.

[13] Wu, X. Q.—Wang, K. Q.: Fuzzy Directional Element Energy Feature (FDEEF) based Palmprint Identification. Proceedings of 16th International Conference, ICPR '02, Vol. 1, Aug. 2002, pp. 95–98.

[14] Kong, W. K.—Zhang, D.: Palmprint Feature Extraction Using 2D Gabor Filters. Pattern Recognition. Vol. 36, 2003, No. 10, pp. 2339–2347.

[15] Zhang, L.—Zhang, D.: Characterization of Palmprints by Wavelet Signatures via Directional Context Modeling. IEEE Transactions on Systems, Man and Cybernetics, Part B, Vol. 34, June 2004, No. 3, pp. 1335–1347.

[16] Wang, X.—Gong, X. H.: Palmprint Identification using Boosting Local Binary Pattern. Proceedings of 18$^{\text{th}}$ International Conference, ICPR '06, Vol. 3, Aug. 2006, pp. 503–506.

[17] Chen, G. Y.—Bui, T. D.: Palmprint Classification using Dual-Tree Complex Wavelets. Proceedings of 13$^{\text{th}}$ International Conference, ICIP '06, Oct. 2006, pp. 2645–2648.

[18] Julia, N.—Gabriele, S.: Dual-Tree Complex Wavelet Transform in the Frequency Domain and an Application to Signal Classification. Technical Report/Department for Mathematics and Computer Science, University of Mannheim, 2003.

[19] Kingsbury, N. G.: The Dual-Tree Complex Wavelet Transform: A New Efficient Tool for Image Restoration and Enhancement. Proceedings of European Signal Processing Conference, Sept. 1998, pp. 319–322.

[20] Kingsbury, N. G.: Shift Invariant Properties of the Dual-Tree Complex Wavelet Transform. Proceedings of International Conference, ICASSP '99, Phoenix, Arizona, USA, Vol. 1, Mar. 1999, pp. 1221–1224.

[21] Kingsbury, N. G.: A Dual-Tree Complex Wavelet Transform with Improved Orthogonality and Symmetry Properties. Processing of International Conference on Image, Sept. 2000, pp. 375–378.

[22] Selesnick, I. W.—Baraniuk, R. G.: The Dual-Tree Complex Wavelet Transform. IEEE Signal Processing Magazine, Vol. 22, 2005, No. 6, pp. 123–151.

[23] Topi, M.— Maricor, S.: Robust Texture Classification by Subsets of Local Binary Patterns. Proceedings of 15$^{\text{th}}$ International Conference, ICPR 2000, Vol. 3, Sept. 2000, pp. 935–938.

[24] Zhao, G.—Pietikainen, M.: Dynamic Texture Recognition Using Local Binary Patterns with an Application to Facial Expressions. IEEE Transactions on Pattern Analysis and Machine Intelligence, Vol. 29, 2007, No. 6, pp. 915–928.

[25] Ahonen, T.—Pietikainen, M.: Face Description with Local Binary Patterns: Application to Face Recognition. IEEE Transactions on Pattern Analysis and Machine Intelligence, Vol. 28, 2006, No. 12, pp. 2037–2041.

[26] Ojala, T.—Pietikainen, M.: A Comparative Study of Texture Measures with Classification based on Feature Distributions. Pattern Recognition, Vol. 29, 1996, pp. 51–59.

[27] Ojala, T.—Pietikainen, M.: Multiresolution Gray-Scale and Rotation Invariant Texture Classification with Local Binary Patterns. IEEE Transactions on Pattern Analysis and Machine Intelligence, Vol. 24, 2002, No. 7, pp. 971–987.

[28] Kong, A.—Zhang D.: Palmprint Identification using Feature-level Fusion. Pattern Recognition, Vol. 39, 2006, No. 3, pp. 478–487.

[29] Zhang, W.— Shan S.: Local Gabor Binary Pattern histogram Sequence (LGBPHS): A Novel Non-Statistical Model for Face Representation and Recogni-

tion. Proceedings of the Tenth IEEE International Conference, ICCV '05, Vol. 1, 2005, pp. 786–791.

[30] Wu, X. Q.—Zhang D.: Palmprint Classification Using Principal Lines. Pattern Recognition, Vol. 37, 2004, No. 10, pp. 1987–1998.

Yanxia Wang received the B. Sc. and M. Sc. degrees from Dalian Polytechnic University, Dalian, China in 1999 and 2003, respectively. She received the Ph. D. degree from the Institute of Information Science, Beijing Jiaotong University, Beijing, China in 2008. Now she is an instructor of College of Mathematics, Physics and Information Engineering, Zhejiang Normal University. Her research interests include image processing, palmprint recognition, etc.

Qiuqi Ruan received the B. Sc. and M. Sc. degrees from Beijing Jiaotong University, China in 1969 and 1981, respectively. From January 1987 to May 1990, he was a Visiting Scholar in the University of Pittsburgh, and the University of Cincinnati. Subsequently, he has been a Visiting Professor in USA for several times. Now he is a Professor, Doctorate Supervisor and the Head of the School of Computer and Information Technology, Northern Jiaotong University. He is also the Head of the Institute of Information Science and the School of Software, Northern Jiaotong University. He is a senior member of IEEE. His main research interests include digital signal processing, computer vision, pattern recognition, virtual reality etc.